

Temperature dependence of Brillouin frequency shift in polymers controlled by plasticization effect

Kazunari Minakawa,^{1,a)} Kotaro Koike,² Qiming Du,³ Neisei Hayashi,¹ Yasuhiro Koike,² Yosuke Mizuno,¹ and Kentaro Nakamura^{1,a)}

¹*Precision and Intelligence Laboratory, Tokyo Institute of Technology, 4259 Nagatsuta-cho, Midori-ku, Yokohama 226-8503, Japan*

²*Keio Photonics Research Institute, Keio University, 7-1 Shinkawasaki, Saiwai-ku, Kawasaki 212-0032, Japan*

³*Polytechnic School of Engineering, New York University, 6 MetroTech Center, Brooklyn, New York 11201, USA*

(Received 30 October 2014; accepted 2 April 2015; published online 14 April 2015)

The temperature-dependence coefficient of Brillouin frequency shift (BFS) in perfluorinated graded-index polymer optical fibers is known to change drastically, because of the glass transition, at a certain critical temperature (T_c), above which the BFS becomes more sensitive to temperature. In this paper, we demonstrate that the T_c value can be adjusted by varying the dopant concentration, which is originally used to form the graded-index profile in the core region. Furthermore, we show that the temperature sensitivity of the BFS is enhanced in the presence of dopant probably because the temperature sensitivity of Young's modulus is increased. The results indicate a big potential of the temperature sensors based on Brillouin scattering with an extremely high sensitivity in a specific desired temperature range. © 2015 AIP Publishing LLC.

[<http://dx.doi.org/10.1063/1.4917533>]

I. INTRODUCTION

Temperature sensors based on Brillouin scattering in optical fibers have attracted a great deal of attention in fields such as structural health monitoring and thermal management, because the sensors can easily be distributed for measurement and maintain a high stability based on frequency information.^{1–6} Conventionally, the sensing heads have been primarily composed of glass optical fibers, which cannot withstand strains over $\sim 3\%$. To overcome this restriction, we have been studying Brillouin-based distributed temperature sensors comprising polymer optical fibers (POFs).^{7–10}

To date, we have succeeded in observing Brillouin scattering in perfluorinated graded-index (PFGI-) POFs, which are composed of cyclic transparent optical polymer (CYTOP[®]),¹¹ and found that the temperature-dependent coefficient of the Brillouin frequency shift (BFS) in PFGI-POFs at room temperature is -4.09 MHz/K at 1550 nm.⁸ The absolute value is approximately 3.5 times that for silica single-mode fibers (SMFs), indicating that PFGI-POFs are potentially applicable for temperature sensors with higher sensitivity. A more interesting result is that with an increase in temperature, the temperature-dependent coefficient of BFS in PFGI-POFs abruptly decreases at ~ 80 °C (hereafter called the Brillouin critical temperature T_c) and the temperature sensitivity considerably increases above T_c .¹⁰

This phenomenon is known to be related to the glass transition of polymer. Several previous works have shown that the temperature dependence of the BFS in polymer materials significantly changes at around the glass-transition temperatures T_g .^{12–15} Thus, if the fiber core has a lower T_g

value than the target temperature range, it should work as an excellent temperature sensor with a higher sensitivity. Although one may concern about the thermal stability of POFs under such conditions, we recently demonstrated that the core layer of POFs is not necessarily required to be in a glassy state to maintain its optical transmission loss as long as the cladding layer is in a glassy state.¹⁶

To obtain a desired T_c (or T_g) value, the first choice is to employ a different kind of polymer as the core. But unfortunately, at this moment, there is no alternative of CYTOP that can transmit light at 1550 nm, where various optical devices required to study the BFS properties are available. Thus, in this study, we focus on another possibility, i.e., addition of dopant. The parabolic refractive index profile of GI-POF is formed by a gradient of dopant concentration. Here, as the dopant, low-molecular-weight organic compounds are utilized so that the dopant is compatible with the base polymer and is diffusible during the fiber fabrication process. In other words, the dopant not only forms the GI profile but also performs as plasticizer. As mentioned above, although the BFS behaviors against the temperature change in different kinds of polymers have been reported, almost no attention has been given to the effect of “plasticizer” on T_c . In addition, the influence of the concentration on the temperature-dependence coefficient of the BFS has never been studied, either.

In this paper, we demonstrate that the T_c values follow the T_g changes caused by the plasticization and clarify the influence of the dopant concentration on the coefficient. The best way would be to directly measure the PFGI-POFs with different known dopant concentrations. However, as such fibers or the raw materials are not commercially available, we prepared poly(2,2,2-trifluoroethyl methacrylate)

^{a)}Authors to whom correspondence should be addressed. Electronic addresses: kminakawa@sonic.pi.titech.ac.jp and knakamura@sonic.pi.titech.ac.jp

(PTFEMA)¹⁷ doped with benzyl benzoate (BB) instead, and estimated the BFS at 1550 nm from the acoustic velocity and refractive index. Although the dopant concentration of GI-POF is generally specified by the refractive index difference between the dopant and core base polymer, this time we changed the dopant concentration from the perspective of T_g control.

II. PRINCIPLES

A. Differential scanning calorimetry and glass-transition temperature

The T_g of a polymer material is generally evaluated using a differential scanning calorimeter (DSC),^{18–20} which is also used to characterize various thermal properties. The DSC records the difference in the heat flow rate to the sample and to the reference, which are placed in identical furnaces, as a function of the furnace temperature. In DSC measurements, both the sample and reference cell are heated at a constant temperature rate, and their temperature difference is measured with two thermocouples. The temperature difference is converted into a differential heat flow rate, which is then plotted as a function of the furnace temperature.

The obtained curve, referred to as a DSC curve, is used to determine the T_g of the sample. In the temperature region with no phase transition, the differential heat flow rate does not significantly change. However, while the polymer shows a phase transition to a rubbery state, the temperature ceases to increase because the heat energy is used for the phase transition, resulting in a drastic drop in the DSC curve. The T_g is defined as the midpoint of the heat capacity transition between the upper and lower points of the deviation from the extrapolated rubber and glass lines.

B. Estimation of Brillouin frequency shift in polymer optical fibers

The incident pump light propagating through an optical fiber undergoes an interaction with acoustic phonons, generating backscattered light with a frequency downshift. This phenomenon is known as Brillouin scattering,²¹ and the amount of the frequency downshift (~ 2.8 GHz at 1550 nm in PFGI-POFs),⁸ referred to as the BFS, is expressed by^{21–23}

$$BFS = \frac{2nv_a}{\lambda_p} = \frac{2n}{\lambda_p} \sqrt{\frac{1 - \sigma}{(1 - 2\sigma)(1 + \sigma)}} \frac{E}{\rho}, \quad (1)$$

where n is the refractive index, v_a is the acoustic velocity, λ_p is the pump wavelength, σ is Poisson's ratio, E is Young's modulus, and ρ is the density; all of the parameters are those in the fiber core. Because n , σ , E , and ρ are dependent on temperature,^{24–27} BFS also shows temperature dependence (among the four parameters, the temperature dependence of E has the most significant influence on that of the BFS in poly(methyl methacrylate)-based (PMMA-) POFs).^{8,28,29} The temperature dependence of

BFS is the fundamental principle of Brillouin-based temperature sensing.^{1–6}

As presented above, the Brillouin scattering in POFs has only been experimentally observed in PFGI-POFs. To estimate the Brillouin properties of POFs based on other polymer materials such as PMMA, which have low-loss windows in the visible region, an ultrasonic pulse-echo technique has been developed.^{30–32} In this scheme, ultrasonic pulses are first launched to a polymer sample. Note that because of the relatively large core diameter of a POF, it makes almost no difference whether the sample used here is fiber or bulk.^{30,32} Then, the waves reflected from the top and bottom surfaces are detected (Fig. 1). Using the time delay Δt of their detection along with the sample length l , the acoustic velocity v_a in the sample can be calculated as

$$v_a = \frac{2l}{\Delta t}. \quad (2)$$

Finally, using Eq. (1), the BFS in the sample can be obtained. By repeatedly performing this measurement on the same sample in degassed water at various temperatures, the BFS dependence on temperature can also be obtained.

III. EXPERIMENTS

A. Preparation of polymer samples

We synthesized five PTFEMA samples with different amounts of dopant by free-radical polymerization in bulk. Monomer mixtures (SynQuest Laboratories) containing the initiator (benzoyl peroxide (BPO); Sigma Aldrich) and the dopant (benzyl benzoate (BB); Sigma Aldrich) were transferred into glass ampoules and subjected to repeated freeze-pump-thaw cycles. In this step, the amount of BB in each monomer mixture was adjusted to range the T_g values of the samples from ~ 35 to ~ 75 °C (samples #1–5). The ampoules were then flame-sealed in vacuo, and the polymerization was performed in an oil bath. The monomers were distilled using a spinning band column; the BPO was recrystallized from a solution of chloroform and methanol, and the BPO was completely dried in vacuo at room temperature. The BB was used as received.

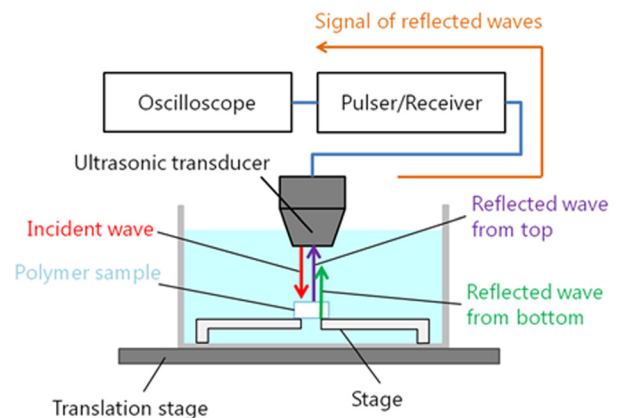


FIG. 1. Schematic of experimental setup for estimating BFS in PTFEMA sample.

B. Differential scanning calorimetry curve

The T_g values of each sample were measured by DSC (DSC-60, Shimadzu). Before the DSC measurements, in order to prevent enthalpy relaxation,¹⁸ we placed the polymer samples at temperatures 30 °C higher than their roughly

estimated T_g values for ~10 min and then rapidly cooled the samples to room temperature. The temperature of the sample chamber was constantly monitored using a thermocouple with a maximal error of ± 0.1 °C. The obtained DSC curves for samples #1–5 are presented as solid lines in Figs. 2(a)–2(e), respectively. The vertical axes were normalized so

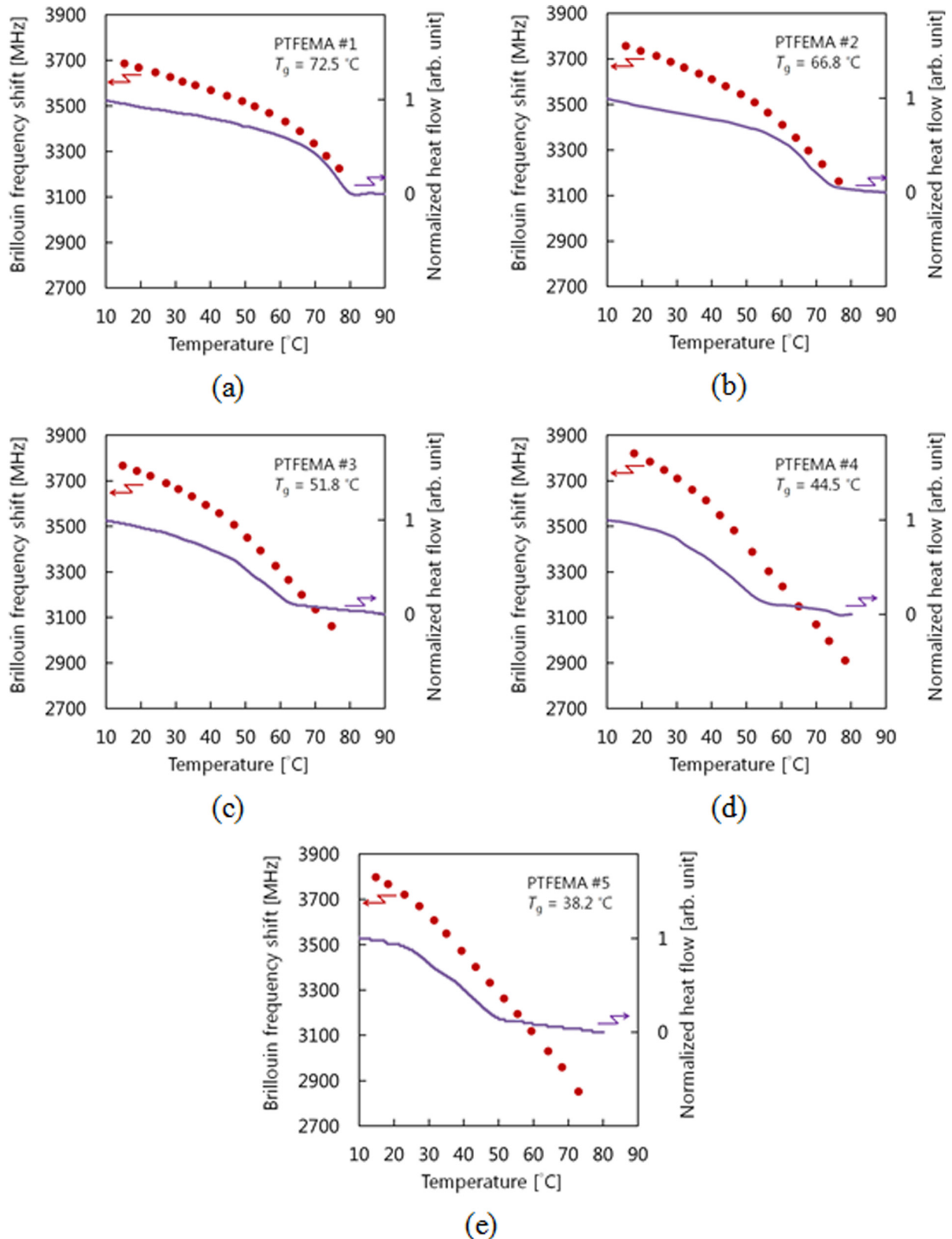


FIG. 2. (a)–(e) Temperature dependence of BFS at 1550 nm (circles) and DSC curves (solid curves) in PTFEMA samples #1–5, respectively.

that the maximal and minimal values in the measured temperature range are 1 and 0, respectively. In all samples, the curves showed an abrupt drop, corresponding to the phase transition. The calculated T_g values of samples #1, #2, #3, #4, and #5 were ~ 72.5 , 66.8, 51.8, 44.5, and 38.2°C, respectively.

C. Brillouin critical temperature

To investigate the BFS dependence on temperature in the PTFEMA samples, the temperature dependence of the acoustic velocity v_a and the refractive index n of each sample must be obtained (See Eq. (1)).

First, the temperature dependence of v_a was investigated using the ultrasonic pulse-echo technique. Each bulk sample was cut into a cylindrical shape with a thickness of 1.50 mm; the top and bottom surfaces were carefully polished with 3- μm alumina powders. To ensure a similar thermal history as that for the DSC-curve measurement, the samples were held at temperature 30°C higher than T_g for ~ 10 min and then rapidly cooled to room temperature. The samples were then placed in degassed water (see Fig. 1) and were irradiated by ultrasonic pulses with a central frequency of 20 MHz, which were generated by a focus-type transducer connected to a pulser/receiver. The v_a values obtained at room temperature for each sample are presented in Table I. Their temperature dependence was then obtained by changing the temperature of the degassed water from 10 to 80°C. The temperature was constantly monitored using a platinum resistance temperature detector with a maximal error of ± 0.4 °C.

Next, we measured the refractive indices of each sample using a prism coupler (Model 2010/M, Metricon) with an accuracy of ± 0.0005 . The probe wavelengths were 532, 632.8, 839, and 1544 nm. The coupling profiles were analyzed as functions of the incident angle. The measured values were fitted to the three-term Cauchy's equation,³³ and the refractive indices at 1550 nm (where the Brillouin properties of PFGI-POFs¹⁰ have been studied) were obtained, as presented in Table I. The refractive indices solely depend on the BB concentration. As reported for PMMA,²⁴ the temperature dependence of the refractive indices was assumed to be negligible.

By substituting the measured values of v_a , n , and λ_p ($=1550$ nm) into Eq. (1), we then calculated the BFS in PTFEMA samples #1–5 at each temperature, which is plotted using circles in Figs. 2(a)–2(e), respectively. The

TABLE I. The dopant (BB) concentration, acoustic velocity at room temperature, and refractive indices of PTFEMA bulk samples.

Sample	BB (mol%)	Acoustic velocity v_a (m/s) at room temperature	Refractive index n at 1550 nm
#1	0	2.01×10^3	1.408
#2	1.99	2.03×10^3	1.415
#3	4.04	2.01×10^3	1.419
#4	6.02	2.04×10^3	1.424
#5	7.98	1.99×10^3	1.426

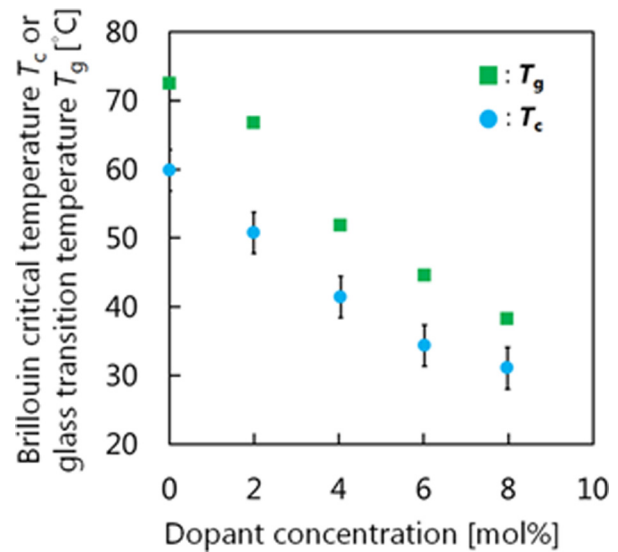


FIG. 3. The T_c (circles) and the T_g (squares) values plotted as functions of the dopant concentration. The error bars of T_c are ± 3 °C.

temperature-dependent coefficients suddenly decreased at the T_c of ~ 66.6 , 55.6, 41.4, 34.0, and 26.2°C in samples #1–5, respectively. These values, calculated using the intersection of two straight lines fitted to the BFS curve in its linear regions at sufficiently low and high temperatures, contain maximal errors of ± 3 °C. Water absorption was negligibly small because each temperature dependence of the BFS was almost identical to that measured when temperature was decreasing from 80°C. Figure 3 shows T_c and T_g plotted as functions of the dopant concentration. With increasing concentration, both T_c and T_g monotonically decreased, and T_c was always lower than T_g by ~ 10 °C, irrespective of the concentration. As far as we know, this is the first observation that T_c exactly follows T_g in a single polymer material when the dopant concentration varies. In Fig. 4, the temperature-dependence coefficients of the BFS at 20°C and ~ 75 °C are

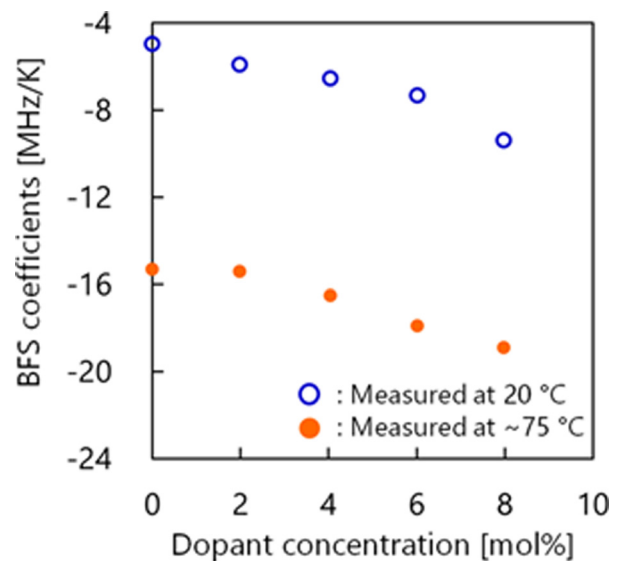


FIG. 4. Temperature-dependence coefficients of the BFS plotted as functions of the dopant concentration; measured at 20°C (blue hollow circles) and ~ 75 °C (orange solid circles).

presented as functions of the dopant concentration. Regardless of whether the temperature is below or above T_c , the coefficients decreased as the dopant concentration increased. For example, at room temperature (20 °C), the BFS coefficient varies from -5.0 to -9.4 MHz/K when the dopant concentration varies approximately from 0 to 8 mol%. This corresponds to 90-% improvement in the temperature sensitivity (the absolute value of the coefficient). While the mechanism is not clear, we believe that the temperature sensitivity of the Young's modulus E in Eq. (1) might increase by the plasticization effect.

IV. CONCLUSION

We prepared five doped PTFEMA samples and studied the influence of the dopant on the temperature dependence of the BFS. The T_c value was experimentally proved to follow the T_g value that was artificially controlled by the dopant concentration. We also found that the absolute values of the temperature-dependence coefficients increase as the dopant concentration increase, probably because the temperature sensitivity of the Young's modulus is increased. These results lead to the conclusion that the doping method is an easy and efficient way to design POF-based Brillouin temperature sensors with extremely high sensitivities in specific desired temperature regions.

ACKNOWLEDGMENTS

This work was partially supported by the Funding Program for World-Leading Innovative R&D on Science and Technology (FIRST), Grants-in-Aid for Young Scientists (A) (No. 25709032) and for Challenging Exploratory Research (No. 26630180) from the Japan Society for the Promotion of Science (JSPS), and by research grants from the General Sekiyu Foundation, the Iwatani Naoji Foundation, and the SCAT Foundation. N. Hayashi acknowledges a Grant-in-Aid for JSPS Fellows (No. 25007652).

¹T. Kurashima, T. Horiguchi, and M. Tateda, *Appl. Opt.* **29**, 2219 (1990).

²T. Horiguchi and M. Tateda, *J. Lightwave Technol.* **7**, 1170 (1989).

³K. Hotate and T. Hasegawa, *IEICE Trans. Electron.* **E83-C**, 405 (2000).

⁴Y. Mizuno, W. Zou, Z. He, and K. Hotate, *Opt. Express* **16**, 12148 (2008).

⁵T. Kurashima, T. Horiguchi, H. Izumita, S. Furukawa, and Y. Koyamada, *IEICE Trans. Commun.* **E76-B**, 382 (1993).

⁶D. Garus, K. Kriebber, F. Schliep, and T. Gogolla, *Opt. Lett.* **21**, 1402 (1996).

⁷Y. Mizuno and K. Nakamura, *Appl. Phys. Lett.* **97**, 021103 (2010).

⁸Y. Mizuno and K. Nakamura, *Opt. Lett.* **35**, 3985 (2010).

⁹K. Minakawa, K. Koike, N. Hayashi, Y. Koike, Y. Mizuno, and K. Nakamura, *IEICE Electron. Express* **11**, 20140285 (2014).

¹⁰K. Minakawa, N. Hayashi, Y. Shinohara, M. Tahara, H. Hosoda, Y. Mizuno, and K. Nakamura, *Jpn. J. Appl. Phys., Part I* **53**, 042502 (2014).

¹¹Y. Koike and K. Koike, *J. Polym. Sci. Part A: Polym. Phys.* **49**, 2 (2011).

¹²E. A. Friedman, A. J. Ritger, and R. D. Andrews, *J. Appl. Phys.* **40**, 4243 (1969).

¹³E. Kato, *J. Chem. Phys.* **73**, 1020 (1980).

¹⁴L. N. Durvasula and R. W. Gammon, *J. Appl. Phys.* **50**, 4339 (1979).

¹⁵Y. Y. Huang and C. H. Wang, *J. Chem. Phys.* **61**, 1868 (1974).

¹⁶H. Yoshida, R. Nakao, Y. Masabe, K. Koike, and Y. Koike, *Polym. J.* **46**, 823 (2014).

¹⁷K. Koike and Y. Koike, *J. Lightwave Technol.* **27**, 41 (2009).

¹⁸S. D. Clas, C. R. Dalton, and B. C. Hancock, *Pharm. Sci. Technol. Today* **2**, 311 (1999).

¹⁹G. W. H. Hohne, W. Hemminger, and H. J. Flammersheim, *Differential Scanning Calorimetry: An Introduction for Practitioners* (Springer-Verlag, Berlin, 1996).

²⁰D. T. Haynie, *Biological Thermodynamics* (Cambridge University Press, Cambridge, 2008).

²¹G. P. Agrawal, *Nonlinear Fiber Optics* (Academic Press, San Diego, 1995).

²²K. F. Graff, *Wave Motion in Elastic Solids* (Dover Publications, New York, 1975), p. 276.

²³T. Horiguchi, T. Kurashima, and M. Tateda, *IEEE Photon. Technol. Lett.* **1**, 107 (1989).

²⁴J. M. Cariou, J. Dugas, L. Martin, and P. Michel, *Appl. Opt.* **25**, 334 (1986).

²⁵R. Kono, *J. Phys. Soc. Jpn.* **15**, 718 (1960).

²⁶M. Fukuhara and A. Sampei, *J. Polym. Sci. Part B: Polym. Phys.* **33**, 1847 (1995).

²⁷J. J. Curro and R. J. Roe, *Polymer* **25**, 1424 (1984).

²⁸M. Silva-Lopez, A. Fender, W. N. MacPherson, J. S. Barton, J. D. C. Jones, D. Zhao, H. Dobb, D. J. Webb, L. Zhang, and I. Bennion, *Opt. Lett.* **30**, 3129 (2005).

²⁹J. Saneyoshi, Y. Kikuchi, and O. Nomoto, *Handbook of Ultrasonic Technology* (Nikkan Kogyo, Tokyo, 1978), Chap. 5.

³⁰N. Hayashi, Y. Mizuno, D. Koyama, and K. Nakamura, *Appl. Phys. Express* **4**, 102501 (2011).

³¹K. Minakawa, N. Hayashi, Y. Mizuno, and K. Nakamura, *Appl. Phys. Express* **6**, 052501 (2013).

³²N. Hayashi, Y. Mizuno, D. Koyama, and K. Nakamura, *Appl. Phys. Express* **5**, 032502 (2012).

³³A. L. Cauchy, *Mémoire sur la Dispersion de la Lumière* (J. G. Calve, Prague, 1836).